International Journal of Thermal Sciences 100 (2016) 248–254

Contents lists available at ScienceDirect

International Journal of Thermal Sciences

journal homepage: www.elsevier.com/locate/ijts

A compact closed-form Nusselt formula for laminar longitudinal flow between *rectangular/square* arrays of parallel cylinders with *unequal* row temperatures

Hamidreza Sadeghifar [a, b, c, *], Ned Djilali [b, d], Majid Bahrami [a]

[a] Laboratory for Alternative Energy Conversion (LAEC), School of Mechatronic Systems Engineering, Simon Fraser University, Surrey V3T 0A3, BC, Canada
[b] Institute for Integrated Energy Systems and Energy Systems and Transport Phenomena Lab (ESTP), University of Victoria, Victoria V8W 3P6, BC, Canada
[c] Department of Chemical and Biological Engineering, University of British Columbia, 2360 East Mall, Vancouver, BC V6T 1Z3, Canada
[d] Department of Mechanical Engineering, University of Victoria, Victoria V8W 3P6, BC, Canada

ARTICLE INFO

Article history:
Received 6 April 2015
Received in revised form
29 September 2015
Accepted 4 October 2015
Available online 11 November 2015

Keywords:
Nusselt number
Heat transfer coefficient
Laminar
Parallel cylinders
Rectangular array
Unequal cylinder temperatures

ABSTRACT

Axial flows over cylinders are frequently encountered in practice, e.g. in tubular heat exchangers and reactors. Using the Integral method, closed-form relationships are developed for heat transfer coefficients or Nusselt number inside a fluid flowing axially between a *rectangular/square* array of parallel cylinders with *unequal* temperatures. The model considers the temperature variations of cylinders from one row to another while assuming the same temperature for all the cylinders in each row. The model could well capture several sets of numerical data, which can be regarded as excellent in light of the simplicity and comprehensiveness of the model. The compact and accurate formulae developed in this work can be readily employed, and also implemented into any software or tools, for the estimation of *Nu* in tubular heat exchangers, fins systems, porous media and composite manufacturing.

1. Introduction

Heat transfer through parallel cylinders or tube assemblies is a problem of considerable interest in a variety of industrial thermal applications such as multi-tubular heat exchangers, fins, porous media and rod-bank generators, to name a few [1–3]. A general, easy-to-use and still accurate model that can predict the heat transfer coefficient under different operating conditions is essential for the modeling and design of such systems.

Considerable attempts have been made to study the heat transfer of a longitudinal flow between parallel cylinders. However, almost all of these studies are confined to either numerical solutions or asymptotic models developed for two limited cases: *square* or *triangular* array of cylinders having the *same* temperatures. Table 1 summarizes all the studies performed on laminar-flow heat transfer to a fluid flowing axially between parallel cylinders.

To the authors' knowledge, and as shown in Table 1, the literature lacks a model for estimating the heat transfer coefficient of a laminar flow inside a *rectangular* array of cylinders. Especially, no model or data is available for axial flow of a fluid between parallel cylinders with *unequal* row temperatures, which is indeed a more realistic case in comparison to the case of equal temperatures of the cylinders. The aim of this study is to develop a general compact analytic model for predicting the heat transfer coefficient of a longitudinal fluid flow passing through a rectangular array of parallel cylinders with unequal row temperatures.

It should be noted that the determination of the exact temperature profile is not the final aim of this study. Here we are interested in finding a closed-form analytic relation for the prediction of the heat transfer coefficient. As a result, the integral method can be useful, as it usually leads to compact, simple and sufficiently accurate relations, especially for estimating wall fluxes and average profiles [7–14]. In turn, we use the integral method as a powerful technique for obtaining approximate still reasonable solutions to rather complex problems with remarkable ease. The basic idea is

* Corresponding author. Laboratory for Alternative Energy Conversion (LAEC), School of Mechatronic Systems Engineering, Simon Fraser University, Surrey V3T 0A3, BC, Canada. Tel.: +1 (778) 782 8587.
E-mail addresses: sadeghif@sfu.ca, hsf@chbe.ubc.ca, hsf@mail.ubc.ca, hamidreza.sadeghifar@ubc.ca (H. Sadeghifar).

http://dx.doi.org/10.1016/j.ijthermalsci.2015.10.004
1290-0729/

Table 1
Review on the works tailored for modeling the heat transfer by laminar axial flow between parallel cylinders: There is no model for the case of unequal cylinders temperatures and/or for *rectangular* arrays of cylinders.

Author(s) & year	Limitations & remarks			
	Array of cylinders	Temperatures of cylinders	Porosity	Type of study
Szaniawski & Lipnicki (2008) [1]	Square	Equal	Very high (>95%)	Analytic (complex series form)
Miyatake & Iwashita (1990) [2]	Square Triangle	Equal	–	Numerical
Antonopoolos (1985) [4]	Rectangle	Equal wall heat flux	–	Numerical
Yang (1979) [5]	Square	Equal	–	Numerical
Sparrow et al. (1961) [6]	Triangle	Equal	–	Analytic, series form

that, from the physics of the system, we assume a general shape of the temperature profile. It must be noted that we are not interested in the precise shape of the temperature profile but rather need to know the heat flux and the average profile of the temperature over the considered domain to calculate the heat transfer coefficient. As mentioned earlier, estimating the average profile and the flux values can be well performed by the integral method. The integral method has been successfully applied to several classical problems such as moving plate and boundary layer [7–14]. However, the use of this method to develop a heat transfer model for the fluid flow between parallel cylinders is a novel approach. In the following sections, the model will be presented in a general form to be also suitable, with only minor changes, to other possible applications such as catalytic reactors and the beds packed with cylindrical materials.

2. Model development

Fig. 1 shows a fluid flowing through parallel cylinders of diameter d and length L extended along the x-direction and spaced in a rectangular array. The spacing between the cylinders centers is H in the vertical (z) direction and is W in the horizontal (y) direction. In this model, contrary to available similar studies as listed in Table 1, W is not necessarily equal to H and these parameters can take different values ($H \geq W$). In other words, the general case of longitudinal flow through a *rectangular* array of parallel cylinders is

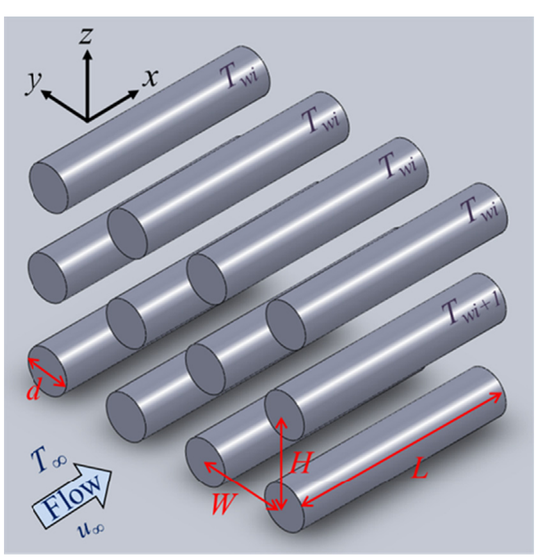

Fig. 1. Fully developed laminar flow between a rectangular array of parallel cylinders; the coordinate system (x,y,z), the fluid temperature and velocity (T_∞ and u_∞), the temperatures of each row of cylinders (T_{wi}: Temperature of all the cylinders in the ith row) and the geometrical parameters W, L, H, and d are shown on figure ($H \geq W$).

considered. The model also assumes fully developed steady state, laminar (creeping) [4,6,14–17] incompressible flow. The physical properties are assumed to be constant, and dissipation, gravity and buoyancy effects are negligible. The cylinders temperatures can change from one row to another ($T_{wi} \geq T_{wi+1}$ where i denotes the row number) but are assumed to be the same in each row. The temperature and velocity of the fluid at the inlet is T_∞ and u_∞, respectively ($T_{w1} > T_\infty$).

Fig. 2 shows the lateral and front views of a longitudinal flow between parallel cylinders and the spacing (δ) between the upper and lower boundaries of the control volume considered:

$$\delta = \begin{Bmatrix} \dfrac{H}{2} & 0 \leq y < \dfrac{W-d}{2} \\ \dfrac{H}{2} - \sqrt{\dfrac{d^2}{4} - \left(\dfrac{W}{2} - y\right)^2} & \dfrac{W-d}{2} \leq y \leq \dfrac{W}{2} \end{Bmatrix} \tag{1}$$

The analytic expression of the velocity profile obtained by Sparrow and Loeffler [18] shows that the velocity is almost uniform except for the area at the vicinity of the cylinders surfaces. This point is also confirmed by the Fluent simulation results shown later in the “Model verification” section. For this reason, the average velocity ($\overline{u}$), which can be readily obtained from the mass flow rate [2,3], is used in the model derivation throughout this study.

The energy equation and the corresponding boundary conditions are ($T(x=0,z) = T_\infty$):

$$\overline{u}\frac{\partial T}{\partial x} = \alpha\left(\frac{\partial^2 T}{\partial z^2}\right) \tag{2}$$

$$T(x, z = +\overline{\delta}) = T_{w1} \tag{3}$$

$$T(x, z = -\overline{\delta}) = T_{w2} \tag{4}$$

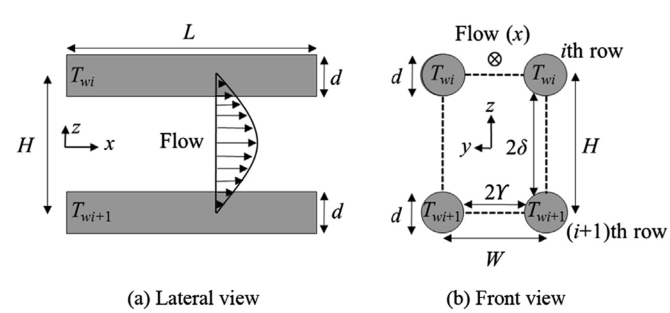

Fig. 2. Front and lateral views of four parallel cylinders with the axial flow; the present model considers the general case of *rectangular* ($H \geq W$) arrays of cylinders which can have unequal row temperatures ($T_{wi} \geq T_{wi+1}$).

where the average value of δ (i.e., $\bar{\delta}$) is used to eliminate the minor, undesired dependency of δ on y for the corners $\left(\frac{W-d}{2} \le y \le \frac{W}{2}\right)$:

$$\bar{\delta} = \begin{Bmatrix} \bar{\delta}_M = \dfrac{H}{2} & 0 \le y < \dfrac{W-d}{2} \\ \bar{\delta}_C = \dfrac{H}{2} - \dfrac{\pi d}{8} & \dfrac{W-d}{2} \le y \le \dfrac{W}{2} \end{Bmatrix} \tag{5}$$

It should be noted that for the space in the range of $0 < y < W - d/2$, the temperature of the fluid on the upper and lower borders (edges) is generally not equal to the temperature of the adjacent cylinders (wall temperatures). As a result, Eqs. (3) and (4) are not accurate for this range of y and the value of the border temperature (subtracted from the wall temperature) must be added to the right-hand sides of Eqs. (3) and (4), even though the border temperature is negligible for packed materials. Here, at first, no border temperature assumption is made to be able to proceed with the modeling. Later, the border temperatures are considered to make the model as accurate as possible, especially for highly porous materials.

In order to solve Eq. (6) with its boundary conditions (Eq. (3) and (4)) using the integral method, the model assumes a parabolic profile for the temperature according to the physics of the problem:

$$T(x,z) = a_0(x) + a_1(x)z + a_2(x)z^2 \tag{6}$$

Solving the model's equations by using the integral method, the final form of the temperature profile is obtained as:

$$\begin{aligned} T(x,z) = &\left[\frac{T_{w1}+T_{w2}}{2} - \left(\frac{T_{w1}+T_{w2}}{2} - T_\infty\right)\exp\left(-\frac{3\alpha x}{\bar{\delta}^2\bar{u}}\right)\right] \\ &+ \left(\frac{T_{w1}-T_{w2}}{2}\right)\left(\frac{z}{\bar{\delta}}\right) + \left(\frac{T_{w1}+T_{w2}}{2} - T_\infty\right) \\ &\exp\left(-\frac{3\alpha x}{\bar{\delta}^2\bar{u}}\right)\left(\frac{z^2}{\bar{\delta}^2}\right) \end{aligned} \tag{7}$$

It should be noted that the fluid temperature is mainly a function of two variables x and z for the rectangular array of cylinders with unequal row temperatures. The variation in the fluid temperature is approximated in the y-direction by dividing the space between the four cylinders (the control volume) into two main and corner blocks as shown in Fig. 3. In turn, considering these two blocks allows accounting for the average temperature variations in the y-direction. However, the temperature gradient at the cylinder wall is later estimated based on a similar quadratic temperature profile obtained for the z-direction.

Similarly to the border velocity profile defined in Refs. [14,15], we consider a border temperature profile based on the average temperature in the case of no border temperature (wall temperatures as boundary conditions) as follows ($0 \le y < \frac{W-d}{2}$ (half of the main block)):

$$\begin{aligned} T_{bor}(x,y) = &\left(\frac{T_{w1}+T_{w2}}{2}\right) + \left(\bar{T}(x) - \frac{T_{w1}+T_{w2}}{2}\right) \\ &\left(\frac{1}{2} - \frac{2y}{W-d}\right)g(\varepsilon) \end{aligned} \tag{8}$$

where $\bar{T}(x)\left(= \int_{z=-\bar{\delta}}^{z=+\bar{\delta}} T(x,z)dz/2\bar{\delta}\right)$ is the average temperature inside the main block, given by:

$$\bar{T}(x) = \left(\frac{T_{w1}+T_{w2}}{2}\right) - \frac{2}{3}\left(\frac{T_{w1}+T_{w2}}{2} - T_\infty\right)\exp\left(-\frac{3\alpha x}{\bar{\delta}^2\bar{u}}\right) \tag{9}$$

And $g(\varepsilon)$ shows the dependency on porosity (ε) [14,15], which is obtained from a linear interpolation between two extreme cases of minimum ($T_{bor} = T_w$) and maximum ($T_{bor} = T_\infty$) possible porosities:

$$g(\varepsilon) = 1.274\varepsilon - 0.274 \tag{10}$$

$$\varepsilon = 1 - \frac{\pi d^2/4}{WH} \tag{11}$$

In order to eliminate the weak, not important dependency of $T_{bor}(x,y)$ on the undesired variable y, we can take an average from that over y to obtain $\bar{T}_{bor}(x)$:

$$\begin{aligned} \bar{T}_{bor}(x) = &\left(\frac{T_{w1}+T_{w2}}{2}\right) + \left(\bar{T}(x) - \frac{T_{w1}+T_{w2}}{2}\right) \\ &\left(\frac{g(\varepsilon)}{2}\right) \quad 0 \le y < \frac{W-d}{2} \end{aligned} \tag{12}$$

Finally, one can reach the temperature profile and its average as:

$$T_B(x,z) = \begin{Bmatrix} T(x,z) + \left(\bar{T}_{bor}(x) - \dfrac{T_{w1}+T_{w2}}{2}\right) & 0 \le y < \dfrac{W-d}{2} \\ T(x,z) & \dfrac{W-d}{2} \le y \le \dfrac{W}{2} \end{Bmatrix} \tag{13}$$

$$\bar{T}_B(x) = \begin{Bmatrix} \bar{T}(x) + \left(\bar{T}_{bor}(x) - \dfrac{T_{w1}+T_{w2}}{2}\right) & 0 \le y < \dfrac{W-d}{2} \\ \bar{T}(x) & \dfrac{W-d}{2} \le y \le \dfrac{W}{2} \end{Bmatrix} \tag{14}$$

The average temperature of the *entire* block can be approximated using:

$$\bar{T}_B(x) = \frac{\int_{z=-\bar{\delta}}^{z=+\bar{\delta}} \int_{y=-W/2}^{y=W/2} T(x,z)dydz}{2\bar{\delta}_M(W-d) + 2\bar{\delta}_C d} \tag{15}$$

The final form of the average temperature will then be:

$$\begin{aligned} \bar{T}_B(x) = &\frac{\left(\frac{T_{w1}+T_{w2}}{2}\right) - \frac{2}{3}\left(\frac{T_{w1}+T_{w2}}{2} - T_\infty\right)\exp\left(-\frac{3\alpha x}{\bar{\delta}_M^2\bar{u}}\right)\left(1 + \frac{g(\varepsilon)}{2}\right)}{1 + \frac{\bar{\delta}_C}{\bar{\delta}_M}\frac{d}{W-d}} \\ &+ \frac{\left(\frac{T_{w1}+T_{w2}}{2}\right) - \frac{2}{3}\left(\frac{T_{w1}+T_{w2}}{2} - T_\infty\right)\exp\left(-\frac{3\alpha x}{\bar{\delta}_C^2\bar{u}}\right)}{\frac{\bar{\delta}_M}{\bar{\delta}_C}\frac{W-d}{d} + 1} \end{aligned} \tag{16}$$

The local heat transfer coefficient can be obtained using:

$$h = \frac{-k\left(\frac{\partial T_B(x,z)}{\partial r}\right)\Big|_{z=\bar{\delta}_C}}{\left(\bar{T}_B(x) - T_{w1}\right)} \tag{17}$$

The term $\left(\frac{\partial T_B(x,z)}{\partial r}\right)_{z=\bar{\delta}_C}$ in the above equation is mathematically calculated as ($r = \sqrt{z^2+y^2}$):

$$\frac{\partial T}{\partial r} = \frac{\partial T}{\partial z}\frac{\partial z}{\partial r} + \frac{\partial T}{\partial y}\frac{\partial y}{\partial r} \tag{18}$$

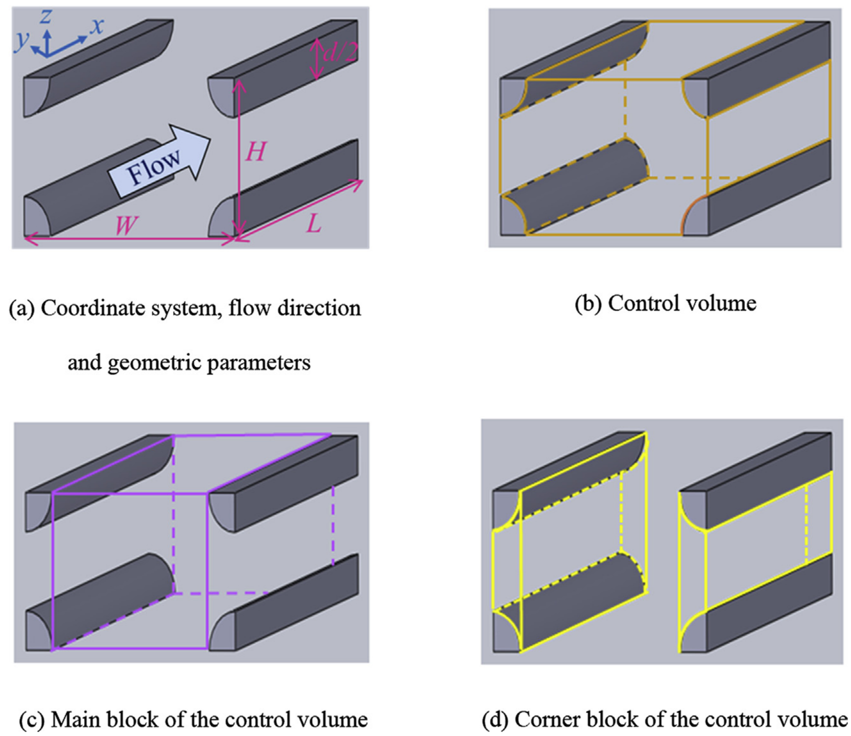

Fig. 3. 3D view of four parallel cylinder quarters considered for the modeling and the space between them considered as the control volume through which the fluid flows.

where the term $\partial T/\partial z$ can be obtained from Eq. (7) and the terms $\partial z/\partial r$ and $\partial y/\partial r$ are:

$$\frac{\partial z}{\partial r}=\frac{z}{\sqrt{z^2+y^2}} \tag{19}$$

$$\frac{\partial y}{\partial r}=\frac{y}{\sqrt{z^2+y^2}} \tag{20}$$

The variation of T along the y-direction was approximated in the present model by defining two main and corner blocks. In order to accurately estimate the T-y slope at the cylinder surface with T_{w1}, according to the physics of the problem and the analytic temperature profile obtained for the z-direction, a quadratic temperature profile similar to Eq. (7) is considered for the y-direction:

$$T(x,y)=\left[T_{w1}-(T_{w1}-T_\infty)\exp\left(-\frac{3\alpha x}{\overline{Y}_C^2\bar{u}}\right)+(T_{w1}-T_\infty)\exp\left(-\frac{3\alpha x}{\overline{Y}_C^2\bar{u}}\right)\left(\frac{y^2}{\overline{Y}_C^2}\right)\right] \tag{21}$$

where $\overline{Y}_C=\frac{W}{2}-\frac{\pi d}{8}$ since $\left(\frac{H}{2}-\frac{d}{2}\right)\le z\le\frac{H}{2}$. It should be noted that the second term of the polynomial temperature has disappeared as the temperatures of the cylinders are the same in each row.

The derivation of temperature with respect to y at the cylinder surface will then be:

$$\frac{\partial T}{\partial y}=(T_{w1}-T_\infty)\exp\left(-\frac{3\alpha x}{\overline{Y}_C^2\bar{u}}\right)\left(\frac{2y}{\overline{Y}_C^2}\right) \tag{22}$$

All the above derivations in Eq. (18) are evaluated at $z=\bar{\delta}_C$ and $y=\overline{Y}_C$.

Knowing $\left(\frac{\partial T(x,z)}{\partial r}\right)_{z=\bar{\delta}_C}$ from the above calculations and $\overline{T}_{Bt}(x)$ from Eq. (16), the local heat transfer coefficient is reached as a closed-form relationship:

$$h=\frac{-Dk}{\bar{\delta}_C\bar{\delta}_M\sqrt{\bar{\delta}_C^2+\overline{Y}_C^2}}\left(\frac{\bar{\delta}_M\bar{\delta}_C(1-F)\left(2A\exp\left(-\frac{3\alpha x}{\bar{\delta}_C^2\bar{u}}\right)+B\right)+\bar{\delta}_C^2F\left(2A\exp\left(-\frac{3\alpha x}{\bar{\delta}_M^2\bar{u}}\right)+B\right)+2\bar{\delta}_M\bar{\delta}_C(T_{w1}-T_\infty)\exp\left(-\frac{3\alpha x}{\overline{Y}_C^2\bar{u}}\right)}{\bar{\delta}_M(W-d)\left(C-\frac{4}{3}A\exp\left(-\frac{3\alpha x}{\bar{\delta}_M^2\bar{u}}\right)\left(1+\frac{g(\varepsilon)}{2}\right)\right)+\bar{\delta}_C d\left(C-\frac{4}{3}A\exp\left(-\frac{3\alpha x}{\bar{\delta}_C^2\bar{u}}\right)\right)-T_{w1}D}\right) \tag{23}$$

where constants A, B, C, D and F are given as below:

$$A=\left(\frac{T_{w1}+T_{w2}}{2}-T_\infty\right) \tag{24}$$

$$B = \left(\frac{T_{w1} - T_{w2}}{2}\right) \tag{25}$$

$$C = T_{w1} + T_{w2} \tag{26}$$

$$D = 2\overline{\delta}_M(W - d) + 2\overline{\delta}_C d \tag{27}$$

$$F = (W - d)/(W\varepsilon) \tag{28}$$

The Nusselt numbers can be obtained using:

$$Nu = \frac{hd}{k} \tag{29}$$

- Special case of equal cylinders temperatures: $T_{wi} = T_{wi+1} = T_w$

Assuming the same temperature for all the cylinders, the local heat transfer coefficient reduces to:

$$h = \frac{-2Dk(T_w - T_\infty)}{\overline{\delta}_C\overline{\delta}_M\sqrt{\overline{\delta}_C^2 + \overline{Y}_C^2}}\left(\frac{\overline{\delta}_M\overline{\delta}_C(1-F)\exp\left(-\frac{3\alpha x}{\overline{\delta}_C^2\overline{u}}\right) + \left(\overline{\delta}_C^2 F\right)\exp\left(-\frac{3\alpha x}{\overline{\delta}_M^2\overline{u}}\right) + \overline{\delta}_M\overline{\delta}_C\exp\left(-\frac{3\alpha x}{\overline{Y}_C^2\overline{u}}\right)}{2\overline{\delta}_M(W-d)\left(T_w - \frac{2}{3}(T_w - T_\infty)\exp\left(-\frac{3\alpha x}{\overline{\delta}_M^2\overline{u}}\right)\left(1 + \frac{g(\varepsilon)}{2}\right)\right) + 2\overline{\delta}_C d\left(T_w - \frac{2}{3}(T_w - T_\infty)\exp\left(-\frac{3\alpha x}{\overline{\delta}_C^2\overline{u}}\right)\right) - T_w D}\right) \tag{30}$$

3. Model verification

Using Fluent Ansys, the axial flow of air with the velocities of 0.5 and 1 m/s is simulated for several rectangular array of cylinders with different row temperatures as shown in Fig. 4. The model predictions are compared to the results (at $x = d$, $7d$ and $14d$) of these simulations in Fig. 5a and b for the model verification for the two velocities. All the fluid properties used for the model verification are listed in Table 2. Fig. 5 shows that the model can well capture the numerical results of the *Nu* in the *fully-developed* region (see Fig. 4) with the maximum and average relative errors of 34 and 16%, respectively. It should be noted that the model error at $x = d$ (the first numerical data shown in Fig. 5a) is 60%, which is much higher than the errors of 27 and 17% obtained for the other two points of $x = L/2$ and $x = L$ ($\overline{u}$=1.0 m/s, $H = 5d$), respectively. The reason for this can be attributed to the fact that the point $x = d$ is within the entrance (non-fully developed) region of the flow. For the fully developed region, the agreement between the closed-form compact formulae of the present study and the numerical data can be regarded as excellent, especially in light of the simplicity and comprehensiveness of the present model. Similar discussions can be made for the other cases considered in Fig. 5.

The numerical data of Ref. [2] provided for the special case of square ($W = H$) array of cylinders with the same temperatures ($T_{wi} = T_{wi+1} = T_w$) can also be used for the verification of the present model. Fig. 6 shows that the model results are in reasonable agreement with the numerical data of Ref. [2] for pitch-to-diameter ($PD = W/d = H/d$) ratios of 2 and 4. For $PD = 1.5$, the model could provide rough, still reasonable, estimations of the *Nu*. The reason for such rough *Nu* estimation (at very low *PD* ratios) by the model can be attributed to the fact that for the packed arrangements ($PD < 1.5$), the velocity profile cannot be approximated to the average velocity. For such cases, the flow may be approximated to a (internal) flow inside a duct or channel.

It should be noted that the analytic model of Ref. [1] developed for the specific case of the *square* ($W = H$) array of *thin* cylinders (very high porosities) with *equal* temperatures ($T_{wi} = T_{wi+1} = T_w$) cannot be used for comparison with the present model. The *Nu* results reported in Ref. [1] shows some inconsistency with the realistic trends of *Nu* with porosity. For instance, with increasing

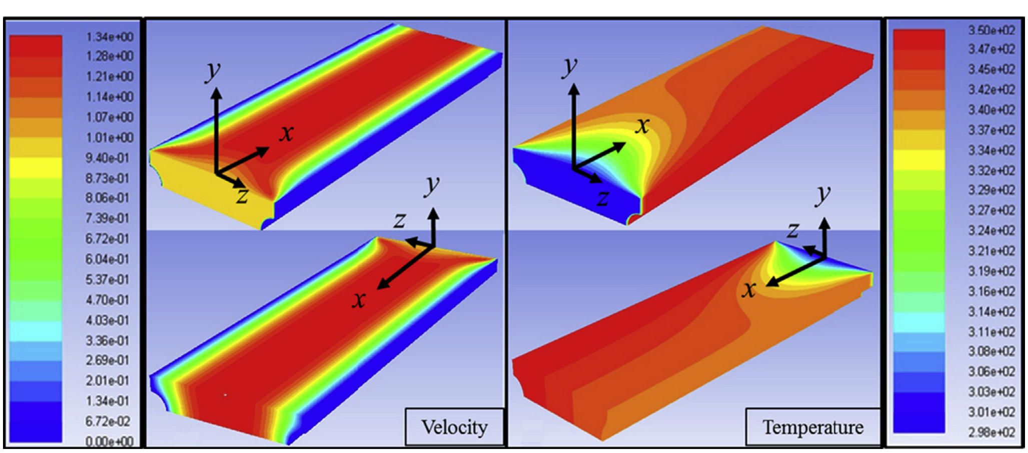

Fig. 4. Temperature (K) and velocity (m/s) contours for the air flowing axially between four cylinders (cylindrical quarters): $L = 14d$, $W = 2d$, $H = 5d$, $d = 8$ µm, $T_{w1} = 350$ K, $T_{w2} = 342$ K, $\overline{u} = 1$ m/s and $T_\infty = 298$ K. Due to the symmetry in the y-direction, half of the space ($0 \le y \le W/2$) has been shown.

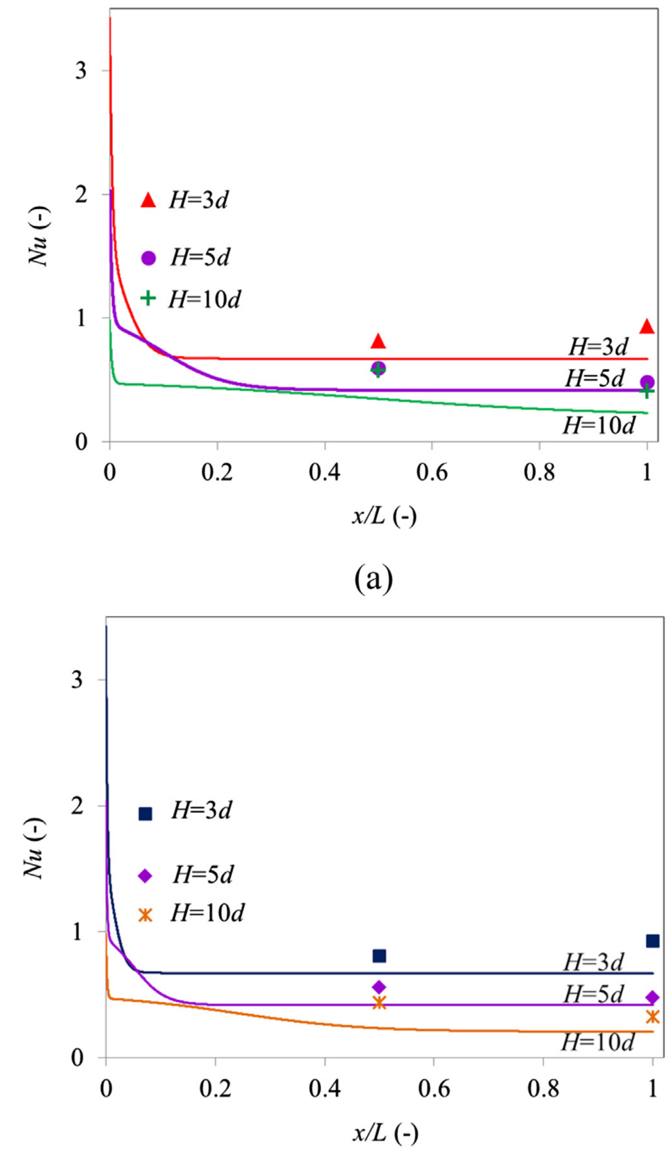

Fig. 5. Comparison of the present model (solid curves) with Fluent Ansys simulations (data points) for the two velocities of: (a) $\overline{u} = 1.0$ m/s and (b) $\overline{u} = 0.5$ m/s. The other parameters are $d = 8$ μm, $L = 14d$, $W = 2d$, $H = 3d$, $5d$ and $10d$, $T_{w1} = 350$ K, $T_{w2} = 342$ K, and $T_\infty = 298$ K.

porosity, the model of Ref. [1] predicts a continuous increase in *Nu*, which is not consistent with the numerical data of Ref. [2].

4. Summary and conclusion

A compact analytic model was developed for predicting the heat transfer coefficient or Nusselt number for longitudinal laminar flow

Table 2
Air thermo-physical properties used for the model validation.

Property	Value	Unit
k	0.024	W/m K
μ	1.7×10^{-5}	Kg/m s
ρ	1.2	Kg/m^3
α	1.99×10^{-5}	m^2/s

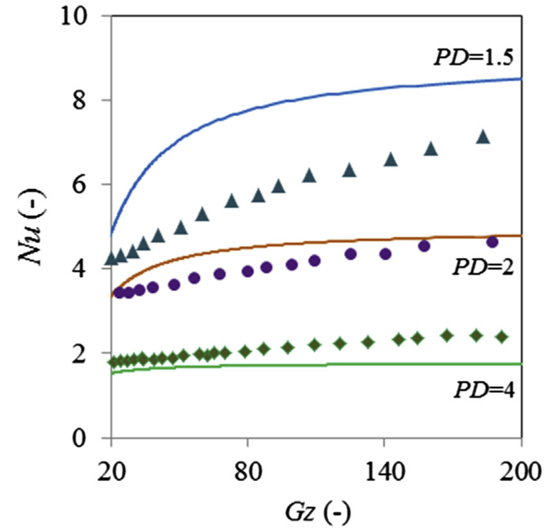

Fig. 6. Comparison of the present model with the numerical results of Ref. [2] for a special case: $d = 1$ mm, $L = 100d$, $W = H = 1.5d$, $2d$ and $4d$ (*square* array of cylinders with the same temperature of $T_w = 350$ K), $\overline{u} = 1$ m/s and $T_\infty = 298$ K.

passing through parallel cylinders. The model accounts for the salient geometric parameters, the fluid thermo-physical properties and the operating conditions. Contrary to all the studies conducted on the longitudinal flow between parallel cylinders, the present model considers the general case of *rectangular* arrays of parallel cylinders whose temperatures can vary from row to row. For such general complex case, the model can accurately predict the *Nu* for any porosity of the tube bank and for any spacings between the cylinders, except for the narrow range of $1 \leq W/d, H/d < 1.5$ where the model gives approximate estimates of the *Nu*. The closed-form simple formulae presented in this study can be readily used for a variety of heat exchangers and rod-generators where longitudinal flows through parallel tubes/pipes are encountered.

References

[1] Andrzej Szaniawski, Zygmunt Lipnicki, Heat transfer to longitudinal laminar flow between thin cylinders, Int. J. Heat Mass Transf. 51 (2008) 3504–3513.
[2] O. Miyatake, H. Iwashita, Laminar-flow heat transfer to a fluid flowing axially between cylinders with uniform surface temperature, Int. J. Heat Mass Transf. 33 (1990) 417–425.
[3] O. Miyatake, H. Iwashita, Laminar-flow heat transfer to a fluid flowing axially between cylinders with uniform wall heat flux, Int. J. Heat Mass Transf. 34 (1991) 322–327.
[4] K.A. Antonopoulos, Heat transfer in tube assemblies under conditions of laminar axial transverse and inclined flow, Int. J. Heat Fluid Flow 6 (1985) 193–204.
[5] I.W. Yang, Heat Transfer and Fluid Flow in Regular Rod Arrays with Opposing Flow, US Department of Energy, 1979.
[6] E.M. Sparrow, A.L. Loeffler, H.A. Hubbard, Heat transfer to longitudinal laminar flow between cylinders, J. Heat Transf. 83 (1961) 415–422.
[7] M.N. Ozisic, Boundary Value Problem of Heat Conduction, International Textbook Company, Scranton, Pennsylvania, 1968.
[8] H. Schlichting, Boundary-layer Theory, seventh ed., McGraw-Hill, New York, 1979.
[9] R.B. Bird, W.E. Stewart, E.N. Lightfoot, Transport Phenomena, second ed., John Wiley & Sons, NJ, 2002.
[10] F.P. Incropera, P.D. Dewitt, Fundamentals of Heat and Mass Transfer, fifth ed., John Wiley & Sons, NJ, 2006.
[11] W. Kays, M. Crawford, B. Weigand, Convective Heat and Mass Transfer, fourth ed., McGraw-Hill, NY, 2005.
[12] L.C. Burmeister, Convective Heat Transfer, second ed., Wiley-Interscience, NY, 1993.
[13] A. Bejan, Convection Heat Transfer, second ed., Wiley-Interscience, 1994.
[14] A. Tamayol, M. Bahrami, Analytical determination of viscous permeability of fibrous porous media, Int. J. Heat. Mass Transf. 52 (2009) 2407–2414.
[15] A.A. Kirsch, N.A. Fuchs, Studies on fibrous aerosol filters — II. Pressure drops in systems of parallel cylinders, Ann. Occup. Hyg. 10 (1967) 23–30.

[16] R. Wiberg, N. Lior, Heat transfer from a cylinder in axial turbulent flows, Int. J. Heat Mass Transf. 48 (2005) 1505–1517.
[17] O.R. Tutty, Flow along a long thin cylinder, J. Fluid Mech. 602 (2008) 1–37.
[18] E.M. Sparrow, A.L. Loeffler Jr, Longitudinal laminar flow between cylinders arranged in regular array, AIChE J. 5 (1959) 325–330.

Nomenclature

A, B, C, D, F: constants defined by Eqs. (24)–(28), respectively
a_0, a_1, *and* a_2: coefficients in the integral method
c_p: heat capacity of fluid J/Kg K
d: cylinder diameter m
Gz: Graetz number $= \rho \overline{u} c_p \frac{d^2}{4} \frac{4(PD)^2-\pi}{k\,x}$ -
h: (local) heat transfer coefficient W/m^2 K
H: spacing between cylinders centers in *z*-direction m
k: fluid thermal conductivity W/m K
L: cylinder length m
Nu: (local) Nusselt number ($=\frac{hd}{k}$) -
PD: pitch-to-diameter ratio ($=W/d = H/d$) for square array of cylinders -
r: radial variable ($=\sqrt{z^2+y^2}$) m
T: fluid temperature K
$\overline{T}$: average fluid temperature K
T_{bor}: border temperature (defined for the main block) K
T_w: cylinder (wall) temperature K
T_{w1}: A constant temperature K
T_{w2}: A constant temperature K
T_{wi}: temperature of all cylinders in *i*th row K
T_{wi+1}: temperature of all cylinders in (i+1)th row K
u: fluid velocity m/s
$\overline{u}$: average fluid velocity m/s
u_∞: velocity of free stream of fluid m/s
W: spacing between cylinders centers in the *y*-direction m
x: coordinate system variable along the flow direction
y: coordinate system variable
z: coordinate system variable

Greek

μ: fluid viscosity Kg/m s
α: fluid thermal diffusivity m^2/s
δ: half of the spacing between the upper and lower boundaries of the control volume m
$\overline{\delta}$: half of the average spacing between the upper and lower boundaries of the control volume m
$\overline{\delta}_C$: $\overline{\delta}$ in the corner block ($=\frac{H}{2}$, see Eq. (5)) m
$\overline{\delta}_M$: $\overline{\delta}$ in the main block ($=\frac{H}{2} - \frac{\pi d}{8}$, see Eq. (5)) m
ε: porosity
ρ: fluid density Kg/m^3
Y: half of the spacing between the left and right boundaries of the control volume m
$\overline{Y}_C$: half of the average spacing between the left and right boundaries of the control volume in the corner block $\left(=\frac{W}{2} - \frac{\pi d}{8}\right)$ m

Subscript

∞: free stream
i: *i*th row of cylinders (i = 1,2,3, …)
B: entire block
bor: border temperature
C: corner part of the block
M: main or middle part of the block
w: wall